Cell Host & Microbe, Volume *23*

Supplemental Information

Listeria Adhesion Protein Induces Intestinal Epithelial Barrier Dysfunction for Bacterial Translocation

Rishi Drolia, Shivendra Tenguria, Abigail C. Durkes, Jerrold R. Turner, and Arun K. Bhunia

SUPPLEMENTAL INFORMATION

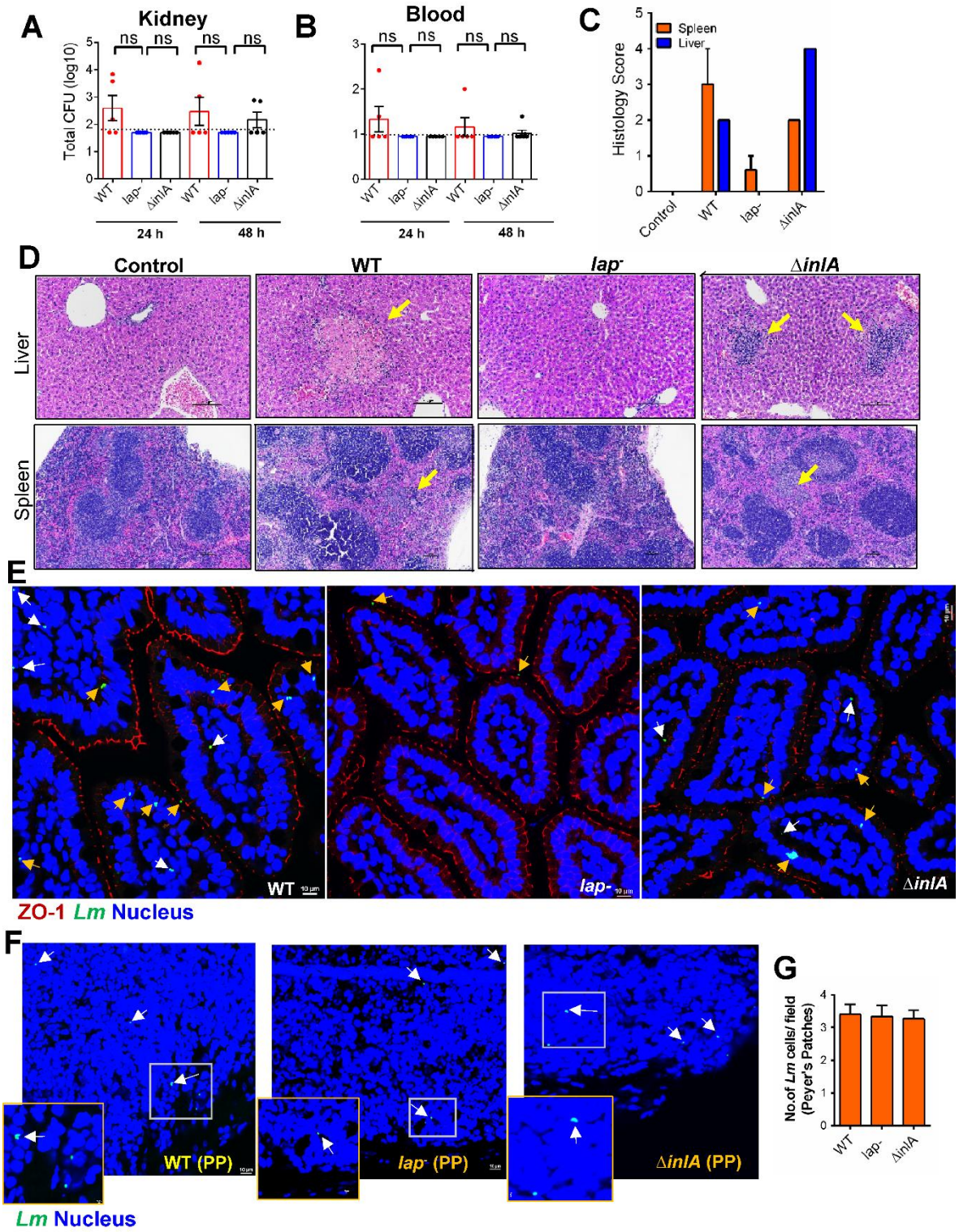

Figure S1. Related to Figure 1. *Listeria* infection and microscopic analysis of tissue sections.

(A,B) The dot plot-showing total CFU obtained from kidney **(A)** and blood **(B)** from 8-10 week-old female A/J mice orally challenged with 1×10^8 CFU of *L. monocytogenes* WT, *lap*$^-$ or Δ*inlA* strains from A/J mice (*n*=5) at 24 and 48 h pi. Bars and brackets represent the mean ± SEM, respectively, from three independent experiments. Dashed horizontal lines indicate the limit of detection for each organ/tissue. Statistical significance was determined by using the Mann-Whitney nonparametric test. ns, not significant.

(C,D) Histology score **(C)** and representative light microscopic images of hematoxylin and eosin stained liver and spleen **(D)**, and from control mice (n=3) or from mice (A/J) orally challenged with 1×10^8 CFU of *L. monocytogenes* WT (n=2), *lap*$^-$ (n=5) or *ΔinlA* (n=2) strains 48 h pi. Arrows (yellow) indicate mild-to-moderate multifocal hepatic necrosis in the livers and multifocal areas of necrosis in the spleen of mice challenged with the WT or Δ*inlA* strain.

(E) Confocal immunofluorescence microscopy of fixed paraffin embedded ileal tissue sections, showing multiple villi, immuno-stained for ZO-1 (red), *Listeria* (green, arrows) and DAPI (blue; nucleus) from WT, *lap*$^-$ or Δ*inlA*-challenged mice 48 h pi. Scale bar, 10 µm. White arrows indicate *L. monocytogenes* detected in the lamina propria of WT and Δ*inlA*-challenged mice. Yellow arrows indicate *L. monocytogenes* detected in the lumen or in the epithelial cells. *L. monocytogenes* (yellow arrows) was detected in the lumen of the *lap*$^-$-challenged mice.

(F,G) Confocal immunofluorescence microscopy of mice Peyer's patches in ileal tissue sections orally challenged with *L. monocytogenes* WT, Δ*inlA* or *lap*$^-$ strains. Scale bar, 10 µm (F). Tissues were fixed and were paraffin embedded, sectioned and immunostained for *Listeria* (green, arrows) and DAPI (blue; nucleus). The inset images show enlargements of the boxed areas. Arrows point to the *L. monocytogenes* presence in the Peyer's patches of WT, *lap*$^-$ *or* Δ*inlA* infected mice (F). Graph representing quantitative measurements of an average number of *L. monocytogenes* (*Lm*) cells in Peyer's patches per examined microscopic field (n=15 fields) from 3 mice for each treatment (G).

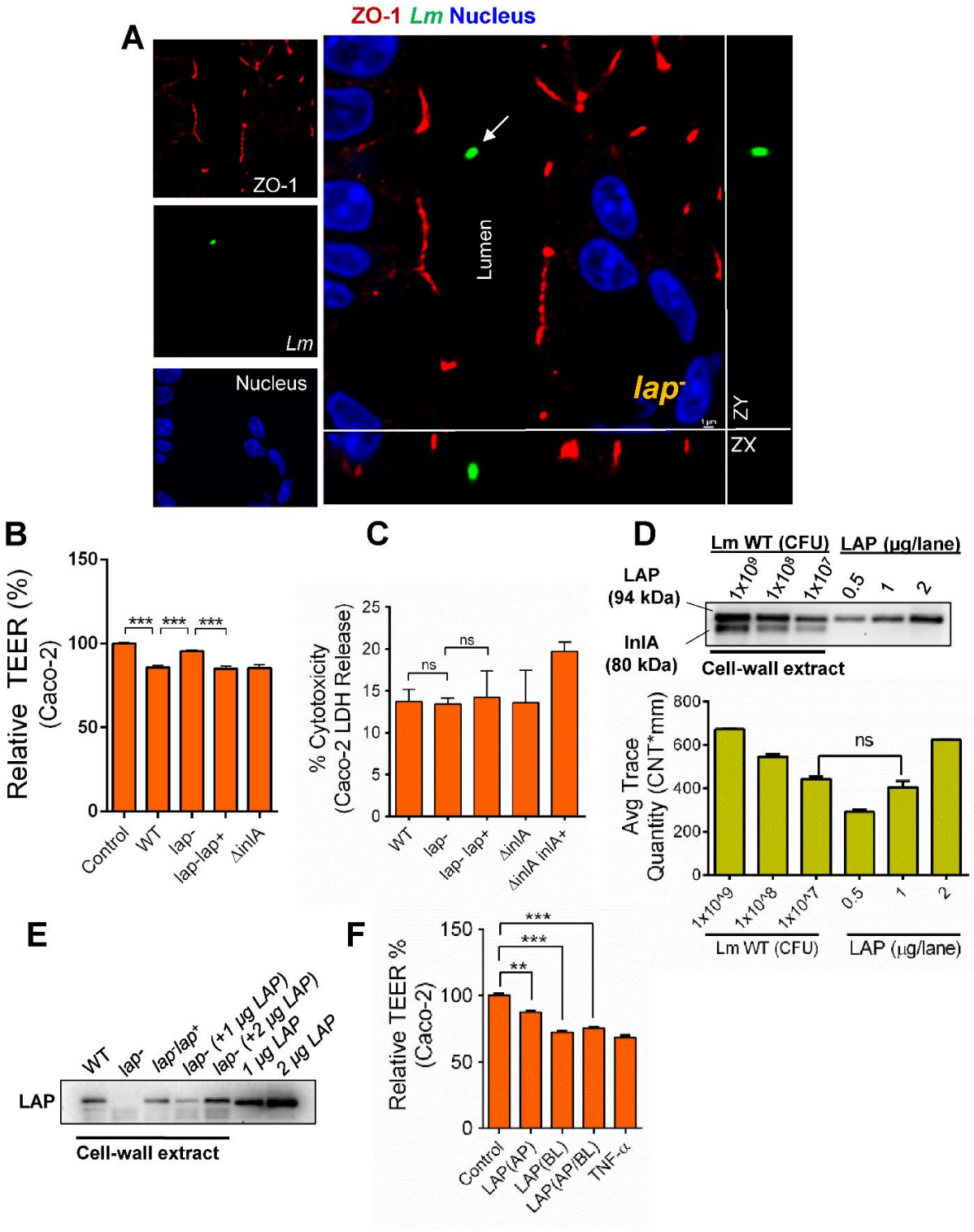

Figure S2. Related to Figure 2. Analysis of tight junction protein (ZO-1) staining, TEER analysis, Caco-2 cell viability by LDH release assay, titration of the relevant concentration of LAP that is available on the bacterial surface and LAP binding to the surface of *L. monocytogenes*.

(A) Confocal immunofluorescence microscopy images of 5 µm thick, ileal tissue sections immunostained for ZO-1 (red), *Listeria* (green, arrows) and DAPI (blue; nucleus) from *lap*$^{-}$ -challenged mice 48 h pi. Scale bars, 1 µm. No *lap*$^{-}$ strain was found to be co-localized with the tight junction protein ZO-1(red). Separated channels are shown individually to the left of the merged images. The X-Z and Y-Z cross-sections were produced by orthogonal reconstructions from the z-stack scanning. Pictures are representative of five different fields from two mice.

(B) Analysis of epithelial permeability by measuring the transepithelial electrical resistance (TEER) across Transwell grown uninfected (control) Caco-2 cells or cells infected apically with *L. monocytogenes* WT, *lap*$^{-}$, *lap*$^{-}$ *lap*$^{+}$ and Δ*inlA* strains (MOI 50, 2 h pi). The data were normalized to uninfected controls and then expressed as the mean % change ± SEM from three independent experiments (n=6). ***, $P<0.001$; **, $P<0.01$, ns, no significance.

(C) Analysis of cell viability by an LDH release assay in culture supernatants of Caco-2 cells infected with WT, *lap*$^{-}$, *lap*$^{-}$ *lap*$^{+}$, Δ*inlA*, Δ*inlA inlA*$^{+}$ strains (MOI 50, 2 h pi) grown on Transwell filter-insert. The data are representative of two independent experiments analyzed in triplicate (n=6) and represent the mean ± SEM. ns, no significance.

(D) Titration of the relevant concentration of LAP that is available on the bacterial surface during infection of Caco-2 cells. (Top panel) Western blot analysis of total LAP and InlA expression in cell wall-associated fractions from $1x10^{9}$, $1x10^{8}$, $1x10^{7}$ CFU of *L. monocytogenes* WT, after 16 h of growth. The anti-LAP mAb-H7 was used to detect LAP and the anti-InlA mAb-2D12 was used to detect InlA. Purified LAP (0.5 µg, 1 µg or 2 µg, as quantified by BCA assay), was used as a standard. (Bottom panel) The mean antibody-reaction intensity values were calculated from measurements of reaction intensity (pixel) for bands. Densitometry report represents the mean ± SEM of three independent experiments. ns, no significance.

(E) Analysis of purified LAP binding to the surface of *L. monocytogenes*. Western blot analysis of cell wall-associated LAP from *L. monocytogenes* WT, *lap*$^{-}$, *lap*$^{-}$ *lap*$^{+}$ strain or *lap*$^{-}$ strain that was incubated with 1 µg or 2 µg of purified LAP for 30 min at room temperature as described in STAR Methods section and analyzed after immunoblotting with the LAP-specific mAb.

(F) Effect of recombinant purified LAP on the filter-insert grown Caco-2 TEER after LAP (1 µg/ml) pre-treatment of the apical (AP), basolateral (BL), or combined apical and basolateral compartments for 48 h. Data represent mean ± SEM from three independent experiments (n=6).

Statistical significance for plots B,C,D, and F was determined by using the one-way ANOVA test followed by a Tukey's multiple comparisons ***, $P<0.001$; **, $P<0.01$; ns, no significance.

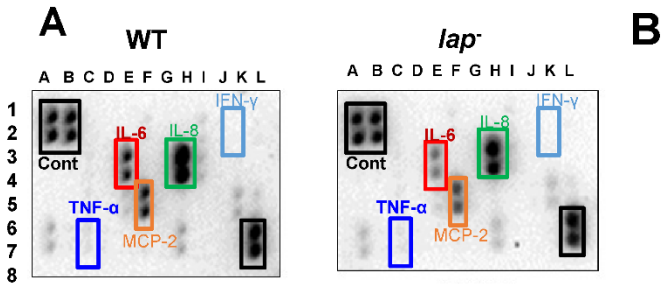

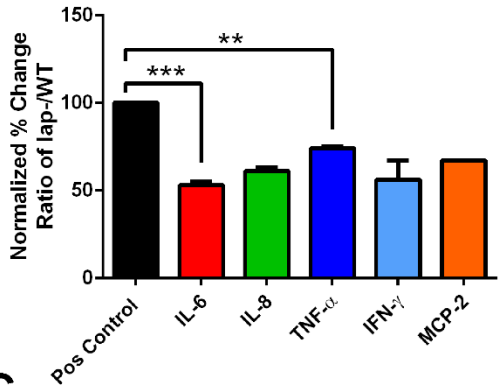

	A	B	C	D	E	F	G	H	I	J	K	L
1	POS	POS	NEG	NEG	Eotaxin 1	Eotaxin 2	G-CSF	GMCSF	ICAM 1	IFN gamma	I-309	IL-1 alpha
2	POS	POS	NEG	NEG	Eotaxin 1	Eotaxin 2	G-CSF	GMCSF	ICAM 1	IFN gamma	I-309	IL-1 alpha
3	IL-1 beta	IL-2	IL-3	IL-4	IL-6	IL-6 sR	IL-7	IL-8	IL-10	IL-11	IL-12 p40	IL-12 p70
4	IL-1 beta	IL-2	IL-3	IL-4	IL-6	IL-6 sR	IL-7	IL-8	IL-10	IL-11	IL-12 p40	IL-12 p70
5	IL-13	IL-15	IL-16	IL-17	IP-10	MCP 1	MCP 2	MCSF	MIG	MIP-1 alpha	MIP-1 beta	MIP-1 delta
6	IL-13	IL-15	IL-16	IL-17	IP-10	MCP 1	MCP 2	MCSF	MIG	MIP-1 alpha	MIP-1 beta	MIP-1 delta
7	RANTES	TGF beta 1	TNF alpha	TNF beta	sTNFRI	sTNFRII	PDGF BB	TIMP 2	BLANK	BLANK	NEG	POS
8	RANTES	TGF beta 1	TNF alpha	TNF beta	sTNFRI	sTNFRII	PDGF BB	TIMP 2	BLANK	BLANK	NEG	POS

C

Time post Treatment	Average % Cytotoxicity (Caco-2)	
	TNF-α	LAP
24 h	4.5 ± 1.0	-5.8 ± 0.3
48 h	2.2 ± 0.5	-3.9 ± 0.4

Figure S3. Related to Figure 3. Comparison of the expression of inflammatory mediators in culture supernatants of Caco-2 cells infected with WT or *lap*⁻ bacteria and analysis of the cytotoxic effect of purified recombinant LAP.

(A,B) (**Top panel**) Array displaying the cytokine (40) expression profiles in Caco-2 cell supernatants infected with *L. monocytogenes* WT (left) or *lap*⁻ (right) using a semi-quantitative membrane-based human inflammation array 3 (Ray Biotech). The array is representative of two independent experiments with each spot in duplicate (n=4). (**Bottom panel**) Map of human inflammation array 3 **(A)**. Bar graph depicting the densitometry analysis of spots corresponding to IL-6, IL-8, TNF-α, IFN-γ, and MCP-2 from arrays **(B)**. The data were normalized to array-specific positive controls and then expressed as the mean % change ± SEM from two independent experiments (n=4).

(C) Analysis of the cytotoxic effect of purified recombinant LAP, if any, on Caco-2 cells. Negative (-) values indicate that % cytotoxicity was less than the untreated control. Human TNF-α (10 µg/ml) was used as a control. The data represent mean (% cytotoxicity) ± SEM (n=6).

Statistical significance for plot B was determined by using the one-way ANOVA test followed by a Tukey's multiple comparisons. ***, $P<0.001$; **, $P<0.01$.

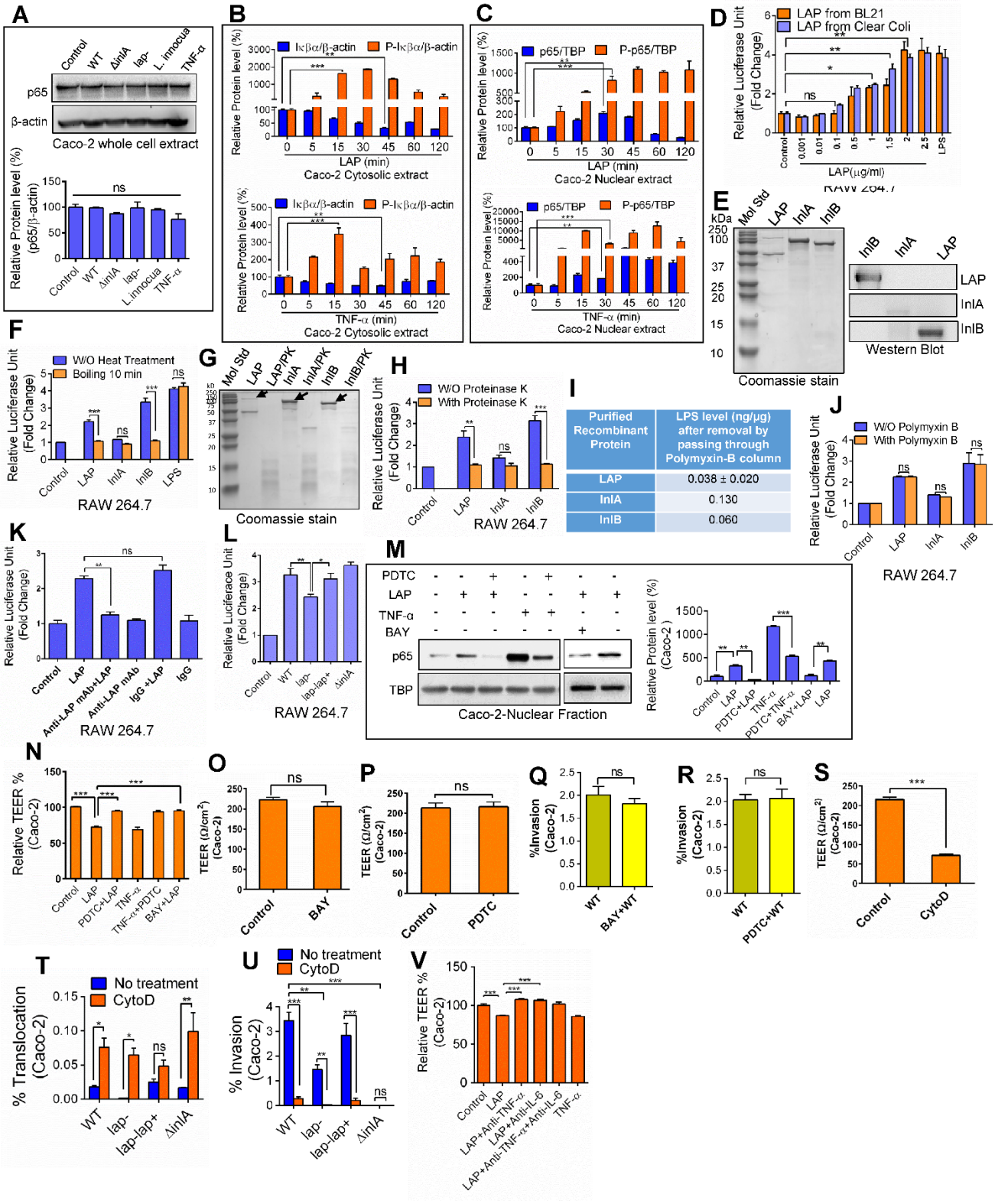

Figure S4. Related to Figure 4. Analysis of LAP-mediated NF-κB activation, and effect of inhibitors on epithelial barrier function and bacterial invasion and translocation in Caco-2 cell model.

(A) Immunoblot analysis showing no marked changes of the total cellular p65 expression levels in the whole-cell lysate of Caco-2 cells infected with *L. monocytogenes* WT, Δ*inlA*, *lap*$^{-}$, and *L. innocua* (MOI 50, 30 min). TBP (TATA-binding protein), uninfected cells (control), and TNF-α (10 ng/ml) were used as loading, baseline, and positive controls, respectively (**top panel).** Densitometry reports of p65 levels after normalization to TBP (**bottom panel**). Immunoblots are representative of 3 independent experiments and densitometry report represent the mean ± SEM of three independent experiments.

(B,C) Densitometry reports of time-dependent IκBα and P-IκBα levels following treatment with purified recombinant LAP (1 μg/ml; **A, top panel**) or TNF-α (10 ng/ml; **B, bottom panel**) in cytoplasmic extract after normalization to the levels of β-actin and p65 and P-p65 following treatment with purified recombinant LAP (1 μg/ml; **C, top panel**) or TNF-α (10 ng/ml; **C, bottom panel**) in nuclear extracts after normalization to the levels of TBP. Densitometry report represents the mean ± SEM of three independent experiments.

(D) Analysis of dose-dependent NF-κB activation by purified recombinant LAP in RAW 264.7 luciferase reporter macrophage cell line. Cells were treated with LAP purified from either from *E. coli* BL21 or ClearColi (1-2500 ng/ml) and LPS (500 ng/ml) for 6 h, and luciferase activity was measured. In Clear Coli, two of the secondary acyl chains of the normally hexa-acylated LPS have been deleted, thus eliminating a key determinant of endotoxicity. The data represent mean ± SEM of three independent experiments (n=6).

(E) Verification of purity and identity of recombinant InlA, InlB and LAP proteins by Coomassie blue staining (top panel) and Western blot (bottom panel). Each well was loaded with 2.5 μg of purified protein in SDS-PAGE (12.5%- polyacrylamide), electrophoretically separated in gel, and Coomassie stained (left panel) or immunoprobed with protein-specific antibodies (top panel). Purified LAP shows two bands. The upper band is the full-length LAP (*lmo1634*, consists of two enzymes, acetaldehyde dehydrogenase (ALDH) and alcohol dehydrogenase (ADH), called alcohol acetaldehyde dehydrogenase) and the lower band (~50 kDa) is predicted to be alcohol dehydrogenase, which tends to separate from the acetaldehyde dehydrogenase when analyzed in SDS-PAGE. Mass-spectrometry analysis of the 50-kDa band reported it as LAP (*lmo1634*).

(F) Analysis of NF-κB activation in RAW 264.7 luciferase reporter macrophage cell line by purified recombinant LAP, InlA or InlB (1 μg/ml each) treated with or without heat treatment (100°C, 10 min). The data represent mean ± SEM of three independent experiments (n=6).

(G) Coomassie blue stained gel showing recombinant (undigested) or proteinase-K digested purified LAP, InlA or InlB proteins.

(H) Analysis of NF-κB activation in RAW 264.7 luciferase reporter macrophage cell line by purified recombinant LAP, InlA or InlB (1 μg/ml each) pre-treated with or without proteinase-K treatment (1 μg/ μg of protein, 30 min, and 37°C). The data represent mean ± SEM of three independent experiments (n=6).

(I) Analysis of LPS (endotoxin) levels in purified recombinant proteins from *E. coli* BL21 after passing through the polymyxin B column. The endotoxin activities in purified recombinant LAP,

InlA and InlB were determined using the LAL Endotoxin Assay Kit. The value for LAP is representative of two independent experiments and is reported as mean of endotoxin level (ng/µg) ± SD). The analysis of InlA and InlB is reported as values from a single analysis.

(J) Analysis of NF-κB activation in RAW 264.7 luciferase reporter macrophage cell line by purified recombinant LAP, InlA or InlB (1 µg/ml each) treated with or without polymyxin B (10 µg/ml) for 1 h prior to exposure to cells for 6 h. The data represent mean ± SEM of three independent experiments (n=6).

(K) Analysis of NF-κB activation of purified recombinant LAP in RAW 264.7 luciferase reporter macrophage cell line by pre-incubating with anti-LAP mAb which reduced luciferase activity, whereas isotype control mouse IgG (1 µg/ml each, 1 h, 37°C) had no effect. The data represent mean ± SEM of three independent experiments (n=6).

(L) Analysis of NF-κB activation in RAW 264.7 luciferase reporter macrophage cell line infected with WT, *lap*$^{-}$, *lap*$^{-}$ *lap*$^{+}$, Δ*inlA* strains (MOI 10, 6 h). Uninfected cells (control) were used as a baseline control. The data represent mean ± SEM of three independent experiments (n=6).

(M) Western blot (**left panel**) showing suppression of LAP-mediated NF-κB activation by NF-κB inhibitors, PDTC or BAY. PDTC (100 µM, 30 min pretreatment) or BAY (10 µM, 30 min pretreatment) significantly reduced the levels of p65 in the nuclear extracts in Caco-2 cells treated with LAP (1 µg/ml, 30 min) or human TNF-α (100 ng/ml, 30 min) compared to the untreated cells. Densitometry reports (**right panel**) of p65 levels after normalization to TBP (loading control) are presented below the immunoblots. Immunoblots are representative of three independent experiments. Densitometry report represent the mean ± SEM of three independent experiments.

(N) Effect of NF-κB inhibitors, PDTC or BAY pre-treatment on TEER of Transwell filter-insert grown Caco-2 cells treated with recombinant purified LAP (1 µg/ml, 24h). Pre-treatment of Caco-2 cells with NF-κB inhibitors, PDTC (100 µM, 30 min, pretreatment) or BAY (10 µM, 30 min, pretreatment) restored LAP-mediated drop in Caco-2 TEER. The data represent the mean ± SEM of three independent experiments (n=3).

(O,P) TEER values of Transwell filter-insert grown Caco-2 cells before and after treatment with NF-κB inhibitors, PDTC (100 µm, 30 min) **(O)** or BAY (10 µm, 30 min) **(P)**. Both NF-κB inhibitors used independently did not affect Caco-2 TEER. The data represent the mean ± SEM of three independent experiments (n=3).

(Q,R) Analysis of *L. monocytogenes* WT invasion of Caco-2 cells pretreated **(Q)** BAY (10 µM, 30 min) or with PDTC (100 µM, 30 min) **(Q)**. Both NF-κB inhibitors did not affect intracellular invasion of *L. monocytogenes* WT. The data represent three independent experiments (n=3).

(S) TEER values for Transwell filter-insert grown Caco-2 cells pre-treated with or without Cytochalasin D (1 µg/ml, for 1 h) (n=3).

(T,U) Analysis of *L. monocytogenes* (WT, *lap*$^{-}$, *lap*$^{-}$ *lap*$^{+}$, Δ*inlA* strains, MOI 50) translocation across **(T)** and invasion into **(U)** Caco-2 cells pretreated with or without cytochalasin D (1 µg/ml, 1 h). The data represent three independent experiments (n=6).

(V) Effect of TNF-α, or IL-6 neutralizing antibodies on TEER of on Transwell filter-insert grown Caco-2 cells treated with anti-TNF-α (1 µg/ml, maintained 24 h during treatment) or anti-IL-6 (1 µg/ml, maintained 24 h during treatment) neutralizing antibodies or added together (n=6). Neutralizing antibodies restored recombinant purified LAP (1 µg/ml, 24 h treatment)-mediated drop in TEER. Recombinant purified LAP was added to the apical side and neutralizing antibodies were added to apical and basolateral side.

Statistical significance for plots A,B,C,D,F,H,J,K,L,M,N,T,U and V was determined by using the one-way ANOVA test followed by a Tukey's multiple comparisons, for plots O,P,Q,R and S using the unpaired t-test. The error bars represent SEM. ***, $P<0.001$; **, $P<0.01$, *, $P<0.05$; ns, no significance.

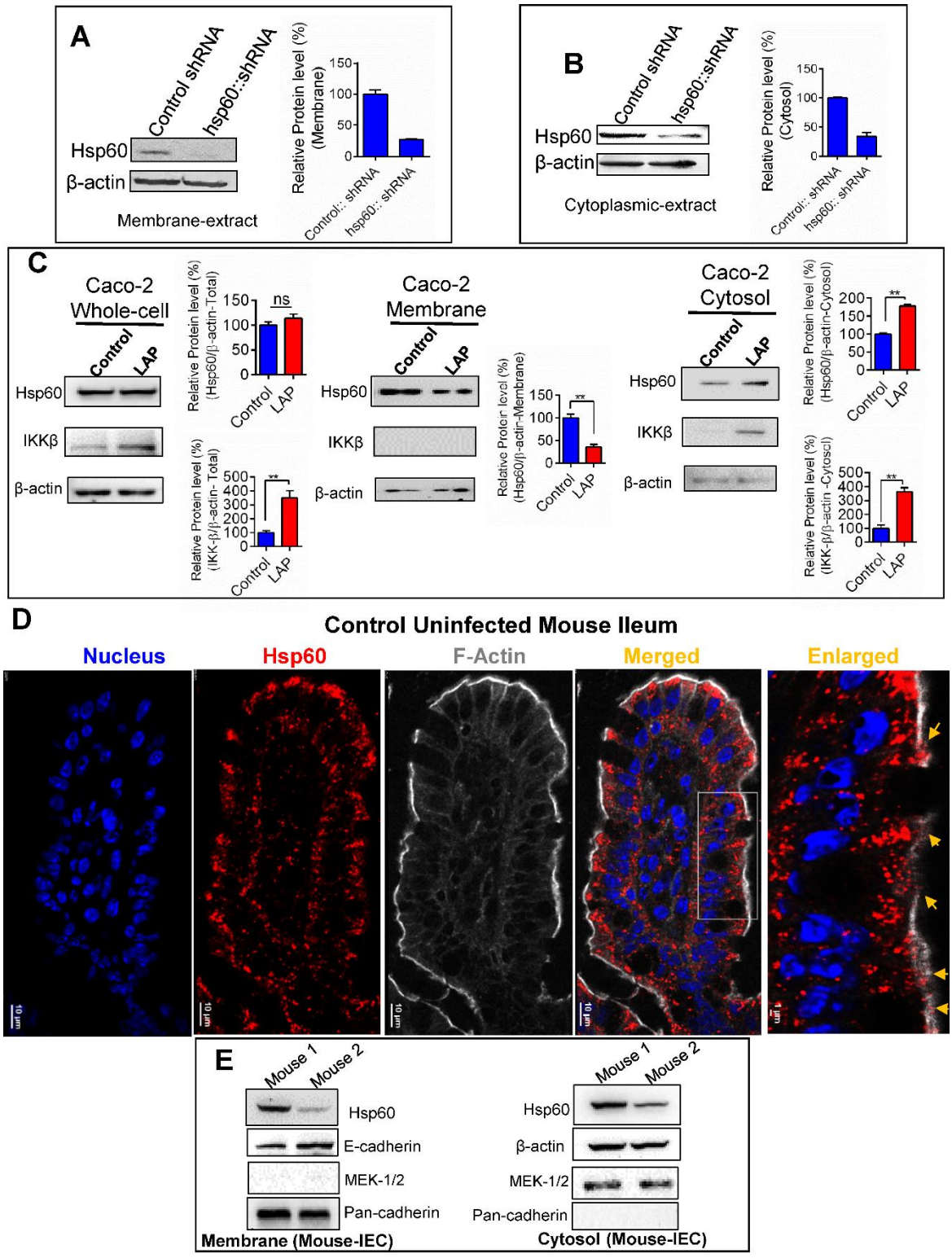

Figure S5. Related to Figure 5. Confirmation of shRNA-mediated Hsp60 knockdown in Caco-2 cells, sub-cellular distribution of IKK-β and Hsp60 proteins in Caco-2 cells and confocal immunofluorescence microscopy and immunoblots for Hsp60 distribution in mouse intestine.

(A,B) Immunoblot analysis confirming Hsp60 knockdown in Caco-2 cells (*hsp60*::shRNA) relative to vector control (control::shRNA) cells. Both membrane **(A)** and cytosolic Hsp60 **(B)** levels was markedly lower (~70%) in Hsp60 knock-down (*hsp60*::shRNA) Caco-2 cells relative to the vector control (control::shRNA) cells. Densitometry reports of Hsp60 levels after normalization to β-Actin from three independent experiments are presented to the right of each blot.

(C) Immunoblot showing the sub-cellular distribution of IKK-β and Hsp60 proteins in the total (left panel), the membrane (middle panel) and the cytosolic (right panel) fractions from Caco-2 cells treated with purified recombinant LAP(1 µg/ml, 30 min) relative to control (untreated) cells. Densitometry reports of protein levels after normalization to β-actin (loading control) is presented to the right of each panel, which represent mean ± SEM of three independent immunoblot experiments. Immunoblot depicts no significant changes in the total Hsp60 levels (left panel), a significant decrease in the membrane Hsp60 levels (middle panel) and a significant increase in the cytosolic Hsp60 (right panel) levels following LAP (1 µg/ml, 30 min) treatment, relative to untreated cells. Immunoblot also shows a significant increase in total (left panel) and cytosolic IKK-β (right panel) protein levels following LAP (1 µg/ml, 30 min) treatment while IKK-β levels were undetectable in the membrane fraction (middle panel).

(D) Confocal immunofluorescence microscopy of ileal tissue sections from uninfected (control) A/J mouse immunostained for Hsp60 (red), F-actin (white, pseudo-color) and DAPI (blue; nucleus). Bars, 10 µm. Separated channels and merged images are shown individually. The far right panel (enlarged) shows enlargements of the boxed areas in the merged image. Bars, 1 µm. Hsp60 was detected apically and in addition to the cytoplasm, in the plasma membrane (arrows, enlarged image) of intestinal epithelial cells, as evidenced by co-localization of Hsp60 (red) with F- actin (white) in the mouse ileal tissue sections. Pictures are representative of five different fields from three mice.

(E) Immunoblot showing the sub-cellular distribution of Hsp60 protein in the membrane (**left panel**), the cytosol (**right panel**) fractions from purified ileal intestinal epithelial cells (IEC) from two representative uninfected (Control) A/J mice. E-cadherin in the membrane fraction (left panel) was used as a positive control. The same extract was probed with antibodies against cytosolic marker MEK-1/2, and membrane marker Pan-cadherin, which confirmed the absence of detectable MEK-1/2 levels in the membrane fraction (**left panel**) and absence of detectable Pan-cadherin levels in the cytosolic fraction (**right panel**).

Statistical significance for panel C was determined by using the unpaired *t*-test. **, $P<0.01$.

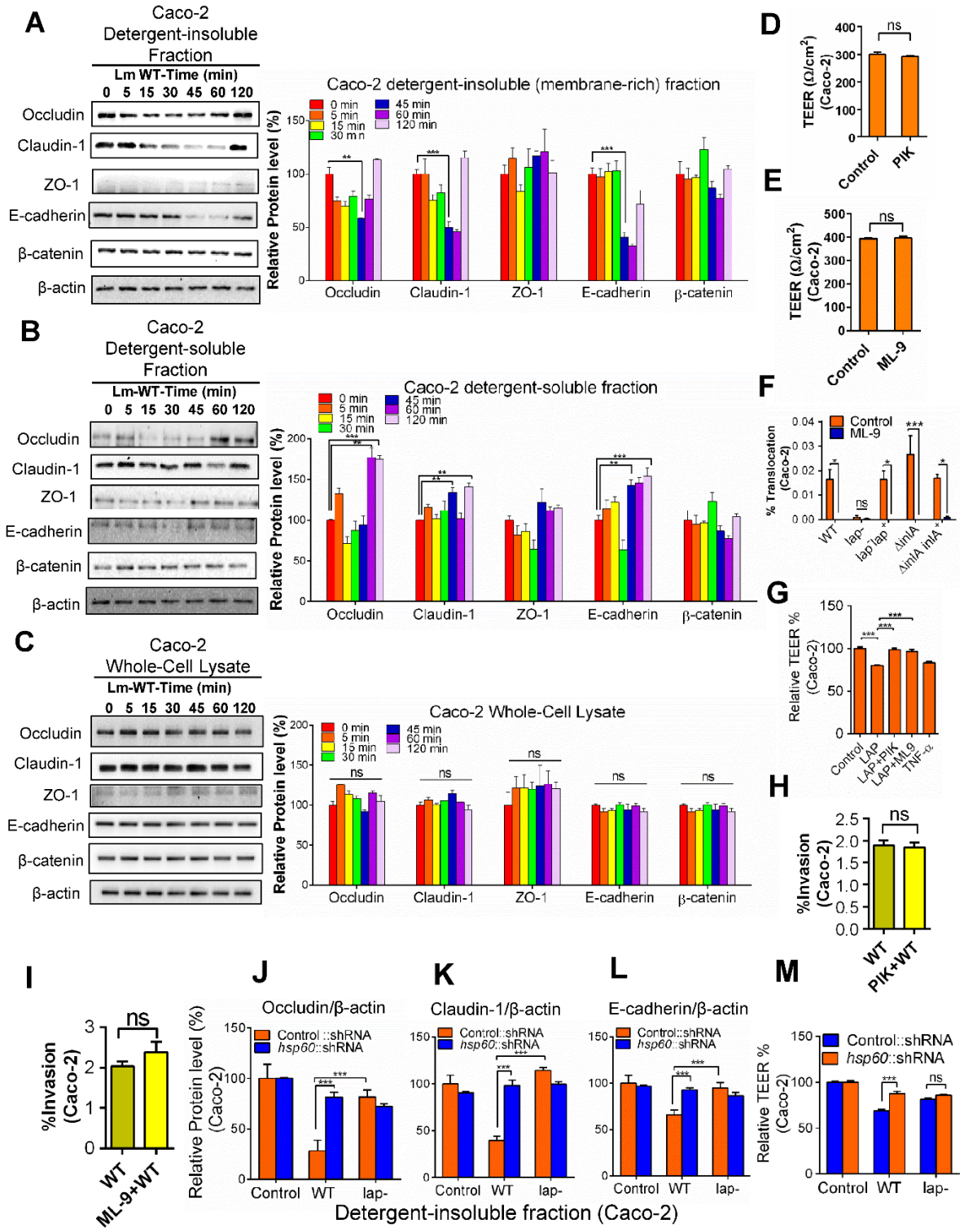

Figure S6. Related to Figure 6. Analysis of transepithelial electrical resistance (TEER) and invasion of *L. monocytogenes* WT strain to Caco-2 cells pretreated with MLCK inhibitor, ML-9, and PIK.

(A,B) Immunoblot showing the time-dependent sub-cellular distribution of TJ (occludin, claudin-1, and ZO-1) and AJ (E-cadherin and β-catenin) proteins in the detergent-insoluble (membrane-rich) **(A)** and detergent-soluble **(B)** fractions from Caco-2 cells infected with the WT strain (MOI 50). Densitometry reports of junctional protein levels after normalization to β-Actin (loading control) is presented in the **right panels** of **A** and **B**, which represent mean ± SEM of three independent immunoblot experiments. Immunoblot shows significant decrease in claudin-1, occludin, and E-cadherin protein expression levels in the detergent-insoluble fractions at 45 min pi (A) and concomitant increase in the expression of claudin-1 and E-cadherin at 45 min pi, and of occludin at 60 min pi in the detergent-soluble fraction (B) relative to uninfected cells (0 min). Immunoblots are representative of three independent experiments.

(C) Immunoblot showing time-dependent analysis of TJ (occludin, claudin-1, and ZO-1) and AJ (E-cadherin and β-catenin) proteins levels in the whole-cell extracts (total protein) from Caco-2 cells infected with the WT strain (MOI 50). Densitometry reports of junctional protein levels after normalization to β-actin (loading control) is presented in the **right panel** of **C** which represent mean ± SEM of three independent immunoblot experiments. Immunoblot shows no significant changes in the levels of occludin, claudin-1 and ZO-1, E-cadherin and β-catenin proteins in the whole-cell lysates during the 120 min time, relative to uninfected cells (0 min). Immunoblots are representative of three independent experiments.

(D,E) TEER values of filter-insert grown Caco-2 cells before and after treatment with MLCK inhibitors, PIK (150 μM, 30 min pre-treatment and maintained during 2-h infection) **(D)** or ML-9 (20 μM, 30 min) **(E)**. Both MLCK inhibitors did not affect Caco-2 TEER. The data are representative of three independent experiments (n=3) and reported as mean ± SEM.

(F) Decreased translocation of the *L. monocytogenes* WT, *lap*$^{-}$ *lap*$^{+}$, Δ*inlA*, and Δ*inlA inlA*$^{+}$ strains, pretreated with MLCK inhibitor, ML-9 (20 μM, 30 min pre-treatment) through Caco-2 cell monolayers grown on Transwell filter-inserts infected at an MOI of 50. The data represent the mean ± SEM of three independent experiments (n=6).

(G) Effect of MLCK inhibitors, PIK (150 μM 30 min pretreatment and maintained during 24 h period) or ML-9 (20 μM, 30 min pre-treatment and maintained during 24 h period) on TEER of Transwell filter-insert grown Caco-2 cells treated with recombinant purified LAP (1 μg/ml). Treatment of Caco-2 cells with MLCK inhibitors, PIK or ML-9 restored LAP-mediated drop in Caco-2 TEER. The data represent the mean ± SEM of three independent experiments (n=6).

(H,I) Analysis of *L. monocytogenes* WT invasion of Caco-2 cells pretreated with MLCK inhibitors, PIK (150 μM, 30 min pre-treatment and maintained during 2-h infection) **(H)** or ML-9 (20 μM, 30 min) **(I)**. Both MLCK inhibitors did not affect intracellular invasion of *L. monocytogenes* WT. The data represent the mean ± SEM of three independent experiments (n=3).

(J-L) Densitometry reports for immunoblots in Fig. 6F showing restoration of occludin **(J)**, claudin-1**(K)** and E-cadherin **(L)** protein levels, in the detergent-insoluble fraction of Caco-2 cells with *hsp60* knocked-down (*hsp60*$^{-}$) infected with *L. monocytogenes* WT or *lap*$^{-}$ strain (MOI 50,

30 min), relative to *L. monocytogenes* WT infected vector control shRNA (control) cells. Densitometry reports represent mean ± SEM of three independent immunoblot experiments.

(M) Analysis of epithelial permeability by measuring the TEER across filter-insert grown vector control Caco-2 cells (Vector Control::shRNA) or with *hsp60* knocked-down (hsp60::shRNA) infected apically with *L. monocytogenes* WT and *lap*$^{-}$ (MOI 50, 2 h). The data were normalized to uninfected controls and expressed as the mean % change ± SEM from three independent experiments, n=6. ***, $P<0.001$; **, $P<0.01$, ns, no significance.

Statistical significance for plots A-C was determined by using the two-way ANOVA test followed by a Dunnett's post hoc test, for plots D,E,H and I by Student *t* test, for plots F,G,J,K,L and M, a two-way ANOVA test followed by a Tukey's multiple comparisons. ****, $P<0.0001$; ***, $P<0.001$; **, $P<0.01$.

SUPPLEMENTAL TABLES

Table S1. Related to Figure 2. Fold change in 40 inflammatory mediators in Caco-2 cells infected with *L. monocytogenes* F4244 (WT) or *lap*$^{-}$ mutant.

Inflammatory Markers	Normalized Fold change in Cytokine Expression levels (Ratio of *lap*$^{-}$/WT)[a]
Eotaxin	0.69 ± 0.05
Eotaxin-2	0.77 ± 0.08
G-CSF	0.72 ± 0.00
GM-CSF	0.73 ± 0.12
ICAM-1	0.70 ± 0.12
IFN-γ	0.56 ± 0.12
I-309	0.46 ± 0.02
IL-1α	0.43 ± 0.01
IL-1β	1.23 ± 0.23
IL-2	0.95 ± 0.12
IL-3	0.79 ± 0.01
IL-4	0.64 ± 0.00
IL-6	0.53 ± 0.02
IL-6 sR	0.64 ± 0.03
IL-7	0.61 ± 0.00
IL8	0.61 ± 0.02
IL-10	0.70 ± 0.10
IL-11	0.52 ± 0.04
IL12-p40	0.55 ± 0.09
IL12-p70	0.41 ± 0.01
IL-13	0.94 ± 0.08
IL-15	0.86 ± 0.05
IL-16	0.74 ± 0.01
IL17	0.67 ± 0.00
IP-10	0.64 ± 0.05
MCP-1	0.69 ± 0.05
MCP-2	0.67 ± 0.00
M-CSF	0.66 ± 0.02
MIG	0.54 ± 0.05
MIP-1-α	0.48 ± 0.04
MIP-1-β	0.62 ± 0.06
MIP-1-δ	0.60 ± 0.03
RANTES	0.93 ± 0.01
TGF-β1	0.89 ± 0.04
TNF-α	0.74 ± 0.01
TNF-β	0.73 ± 0.08
sTNF-RI	0.59 ± 0.01
sTNF RII	0.56 ± 0.05
PDGF-BB	0.57 ± 0.07
TIMP-2	0.61 ± 0.09

[a]The results are expressed as the ratio of *lap*$^{-}$/WT using semi-quantitative membrane-based RayBio human (RayBiotech Inc.) immunoassay. The intensity of signals was quantified by densitometry from two independent experiments (n = 4) and is reported as fold differences ± SD.

Table S2. Related to Star Methods. qRT-PCR primers used in this study.

Gene	**Oligonucleotide sequence (5'-3')**	**References**
TNFα (Mouse)	(F)AATGGCCTCCCTCTCATCAGTT (R)CCACTTGGTGGTTTGCTACGA	(Gilbert et al., 2012)
IL-6 (Mouse)	(F)CAAAGCCAGAGTCCTTCAGAGAGATAC (R)GGATGGTCTTGGTCCTTAGCCAC	(Gilbert et al., 2012)
Gapdh (Mouse)	(F)GGTGGGTGGTCCAAGGTTTC (R)TGGTTTGACAATGAATACGGCTAC	(Gilbert et al., 2012)